# Formation of Asymmetric Bowl-Like Mesoporous Particles via Emulsion-Induced Interface Anisotropic Assembly

Bu Yuan Guan, Le Yu, and Xiong Wen (David) Lou*

School of Chemical and Biomedical Engineering, Nanyang Technological University, 62 Nanyang Drive, Singapore 637459, Singapore

S Supporting Information

ABSTRACT: Mesoporous colloidal particles with tailored asymmetric morphologies and radially oriented large channels are of great importance for development of new carriers for nanoencapsulation, high-performance mass transport nanosystems, and complex assembly structures. However, controllable anisotropic growth to asymmetric mesoporous particles is very challenging via the universal surfactant-directed soft-templating method. Herein we report a simple emulsion-induced interface anisotropic assembly approach to synthesize bowl-like mesoporous polydopamine particles with diameter of ∼210 nm, well-controlled radially oriented mesochannels, and large pore size of ∼11 nm. This interface-driven approach also creates opportunities for tailoring the assembly and formation of various asymmetric and symmetric polydopamine particles. Bowl-like mesoporous carbon particles with radially oriented channels, high accessible surface area of 619 m^2 g^{-1}, and large pore size of ∼8 nm can be fabricated by subsequent hydrothermal treatment and calcination under nitrogen atmosphere. Lastly, we demonstrate that the as-derived bowl-like mesoporous carbon particles manifest enhanced electrocatalytic performance for oxygen reduction reaction in alkaline electrolyte.
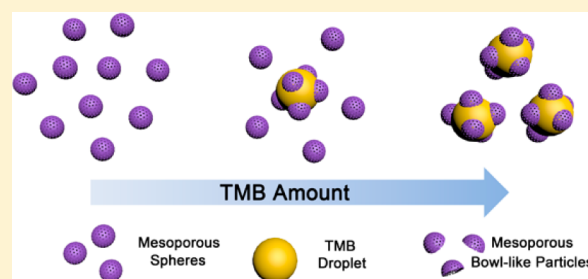
INTRODUCTION

Fabrication of asymmetric particles with ordered internal structures offers a platform for construction of complex particles and ultimately functional nanodevices.[1−5] Going beyond symmetric particles, asymmetric particles with broken centrosymmetry offer not only complex morphologies and structures but sometimes new or enhanced properties due to the anisotropic effects.[6] As a class of asymmetric structures, bowl-like particles have recently drawn attention because of their potential utilizations in energy storage, photonics, and biomedical applications.[7−12] In particular, edible polymer or carbon particles of this shape are of great interest due to their fascinating features such as structural stability, biocompatibility, and electrical conductivity.[13−15] However, most bowl-like particles by other methods are nonporous, which greatly limits the utilization of their internal matrix.

Mesoporous materials with systematically tailored pore architecture are an important class of porous materials.[16] During the past decades, mesoporous colloidal particles play important roles in encapsulation of molecules or nanoparticles with enhanced mass transport. These two features make them widely used in heterogeneous catalysis,[17,18] controlled release of drugs,[19,20] removal of pollutants,[21] protection of biologically active species,[22] and many other applications.[23] However, the size of the guest materials that can be loaded in the mesopores and the efficiency of mass transport through the porous structures are quite restricted by the diameter and structure of mesopores. These limitations might be overcome if large mesochannels were synthesized in a three-dimensional open configuration with respect to the particle surface.[24] Moreover, integration of advantages of both asymmetric and mesoporous features may create new materials for a wide range of applications.

Current approaches to mesoporous nanoparticles with large mesopores (>5 nm) mainly rely on the simple and universal soft-templating method[25−27] using hydrophobic organic additives as pore swelling agents in emulsion systems. However, despite the presence of a large amount of emulsion droplets in the reaction system, only symmetric mesostructured particles can be fabricated via cooperative assembly process because of low interaction between the precursors and hydrophobic organic droplets.[28] Recently, novel mesostructured polydopamine spheres have been prepared via the self-assembly of block copolymer−polydopamine composite micelles.[29] Because dopamine molecules with both catechol and amine groups can effectively bind with most organic and inorganic surfaces,[30] appropriate control of the interaction between emulsion droplets and in situ formed mesostructured polydopamine particles may offer opportunities for the formation of asymmetric mesoporous particles via island nucleation and anisotropic growth mode.[31]

Here, we demonstrate a novel emulsion-induced interface anisotropic assembly strategy to fabricate uniform bowl-like

mesoporous polydopamine and carbon particles with radially oriented large mesochannels. The process starts with the interface formation between two immiscible liquids [1,3,5-trimethylbenzene (TMB) and water] in an emulsion system, and island-shaped mesostructured polydopamine seeds assembled by block copolymer F127/TMB/polydopamine composite micelles will form at the TMB/water interface. Continuous cooperative assembly drives the oriented growth of mesochannels from the initially formed composite micelles along the radial direction within the particles. This seed-mediated anisotropic growth process yields bowl-like mesoporous polydopamine particles with radially oriented mesopores (Figure 1 and Figure S1, Supporting Information (SI)),
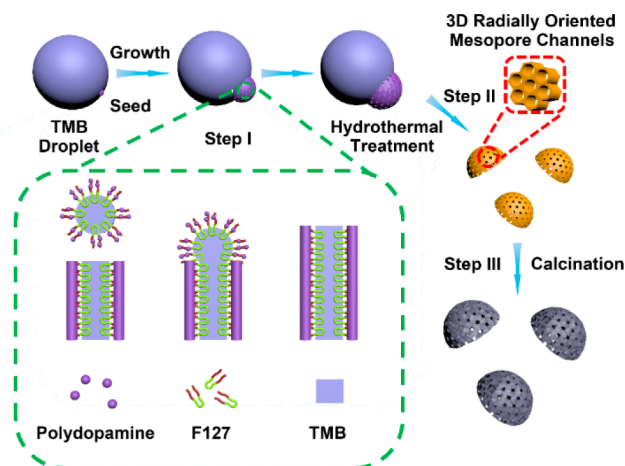

Figure 1. Schematic illustration of the formation process of bowl-like mesoporous particles. Step I, formation of the block copolymer F127/TMB/polydopamine oligomer composite micelles and emulsion-induced interface anisotropic assembly of asymmetric bowl-like mesostructured polydopamine particles with radially oriented large mesochannels. Step II, hydrothermal treatment of the mesostructured polydopamine nanocomposites to stabilize the structure. Step III, carbonization at 800 °C for 2 h under nitrogen atmosphere to generate bowl-like mesoporous carbon particles with radially oriented mesochannels.

and their derived carbon particles can be obtained by subsequent hydrothermal treatment and calcination under nitrogen atmosphere. The resultant bowl-like mesoporous carbon particles manifest enhanced electrocatalytic performance for oxygen reduction reaction (ORR) in alkaline electrolyte. This novel strategy for creating the interface between two immiscible liquids and controlling the interactions between the emulsion droplet and the in situ formed particles will inspire new synthetic designs for functional materials.

■ RESULTS AND DISCUSSION

Field-emission scanning electron microscopy (FESEM) and transmission electron microscopy (TEM) images (Figure 2a,b) show that the formed bowl-like mesoporous polydopamine particles are quite uniform with diameter of ~210 nm. Close observation of the bowl-like particles at a higher magnification (Figure 2c) reveals that the mesochannels are arranged radially from the center to the surface. The center-to-center distance between two adjacent mesochannels is ~21 nm, and the pore size is estimated to be ~11 nm. The cylindrical open channels exposed on the particle surface are clearly shown in Figure 2d. Observed from the side of the mesoporous nanoparticle
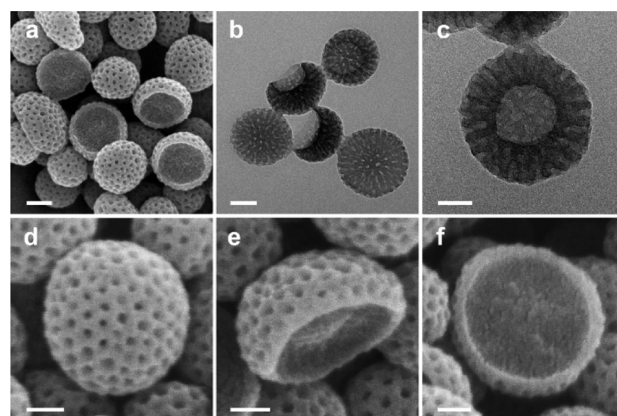
Figure 2. Microscopy characterizations of bowl-like mesoporous polydopamine particles: (a) FESEM image; (b) TEM image; (c) magnified TEM image showing an individual bowl-like particle with radially oriented mesochannels; FESEM images showing (d) spherical face, (e) side face, and (f) sectional face. Scale bars are 100 nm (a, b) and 50 nm (c–f).

(Figure 2e), the bowl-shaped morphology can be further demonstrated. While the sectional face is nonporous, disordered crumples can be found on the whole face (Figure 2f), suggesting that disordered mesostructured polydopamine seeds are formed on the TMB droplet in the initial stage of nucleation process.

The formation of these bowl-like mesoporous polydopamine particles is mainly based on the cooperative formation of block copolymer F127/TMB/polydopamine composite micelles and simultaneous island nucleation and anisotropic growth on the surface of emulsion droplet templates. Figure 3a schematically illustrates the structural evolution of the mesoporous polydopamine nanoparticles prepared with different amounts of organic pore swelling agent. To understand the formation and evolution process, FESEM is used to characterize the mesoporous products collected by using different amounts of
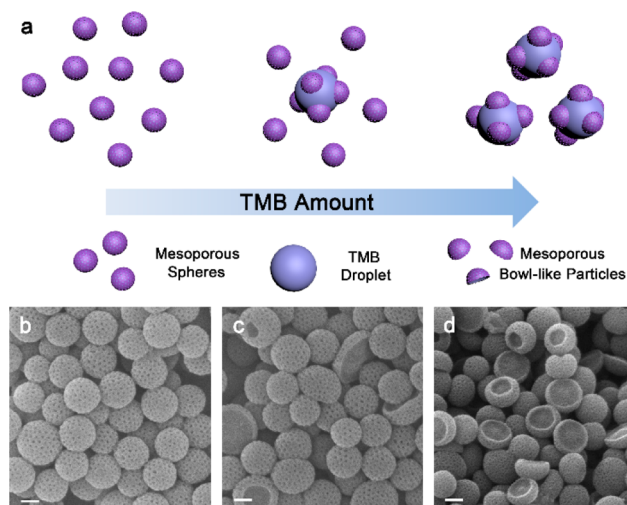
Figure 3. Controllable isotropic and anisotropic growth of mesoporous polydopamine particles. (a) Schematic representation of emulsion-induced interface anisotropic formation of bowl-like mesoporous polydopamine particles in the emulation system. FESEM images of mesoporous particles prepared with different amounts of TMB: (b) 0.16 mL, (c) 0.18 mL, and (d) 0.20 mL. The scale bars are 100 nm.

TMB. By simply increasing the TMB concentration in the reaction system, the product of the mesoporous polydopamine nanoparticles can be continuously tuned from only symmetric nanospheres, to a mixture of nanospheres and bowl-like particles, and finally to solely asymmetric bowl-like particles (Figure 3b−d and Figure S2, SI). This variability in the product verifies that the TMB droplet acts as template for the island nucleation and anisotropic growth of polydopamine nano-particles. This process is quite similar to Volmer−Weber growth mode,[31−33] through which the growth material (for example, metal) often forms segregated islands on the seed nanoparticles (for example, oxide or semiconductor) to reduce the amount of interface. The importance of the pore swelling agent TMB and surfactant F127 in the formation of asymmetric mesoporous particles with large mesochannels is further confirmed by preparing polydopamine particles in the absence of TMB or F127. Without the addition of TMB during the synthesis, aggregated solid polydopamine spheres are formed, and the mesostructure of those derived carbon spheres appears unclear after carbonization in nitrogen atmosphere (Figure S3, SI). Similar nonporous aggregated polydopamine particles are obtained without the addition of F127 in the reaction system (Figure S4, SI).

The growth mode of polydopamine particles can also be continuously varied by adjusting the concentration of the cosolvent (ethanol) in the reaction system. By continuously increasing the volume fraction of ethanol from 0% to 20% then to 40%, we can tune the morphology of the formed mesostructured polydopamine particles from irregular shaped hemispherical nanoshells, to a mixture of round plate-shaped nanoshells and bowl-like nanoparticles, to totally asymmetric bowl-like nanoparticles (Figure S5a−f, SI). The reason for the variability in the growth mode may be that the presence of ethanol slows the polymerization rate of dopamine,[34] which is favorable for the formation of well-defined morphology and mesophases.[28] When the volume fraction of ethanol is increased to 60% and 80%, nonporous particles with bowl-shaped and spherical morphologies, respectively, are formed (Figure S5g−j, SI). This is because the high concentration of ethanol significantly increases the difficulty to form meso-structures[16] and even completely breaks down the emulsion when volume fraction is increased to 80%.

Furthermore, the effect of temperature on morphology and mesostructure is investigated under the same synthetic conditions of bowl-like mesoporous polydopamine particles. By increasing the temperature to 50−70 °C, the diameters of the resultant mesoporous nanoparticles become smaller compared with that of bowl-like particles prepared at room temperature. The morphology of the formed mesostructured polydopamine particles is continuously varied from bowl-like particles to a mixture of bowl-like particles and nanospheres then to totally nanospheres (Figure S6a−c, SI). Moreover, some particles with much larger mesopores than the others have been observed in the samples prepared at 60 and 70 °C. These variabilities in the growth mode and mesostructure are probably because the interaction between water and poly-(propylene oxide) (PPO) segments of block copolymer F127 is reduced as the temperature increases, and more TMB molecules can enter the hydrophobic PPO core to form larger micelles,[28] which significantly decreases the amount of TMB droplet templates in the reaction system. When the temper-ature is increased to 80 °C, nonporous polydopamine particles are formed (Figure S6d, SI). This is perhaps because the

temperature applied is above the critical micelle temperature of F127/TMB/polydopamine composite micelles.

Polydopamine can be transformed into N-doped carbon with a good yield at high temperature.[29] The thermogravimetric analysis (TGA) result indicates that the carbonization process of polydopamine starts at around 300 °C (Figure S7, SI). Therefore, a two-step thermal treatment is employed with pyrolysis of mesoporous polydopamine particles at 300 °C for 3 h and then carbonization at 800 °C for 2 h under nitrogen atmosphere. Bowl-like mesoporous carbon particles and symmetric mesoporous carbon nanospheres are directly produced by carbonization of their corresponding polydop-amine precursors (Figure 4 and Figure S8, SI). FESEM images
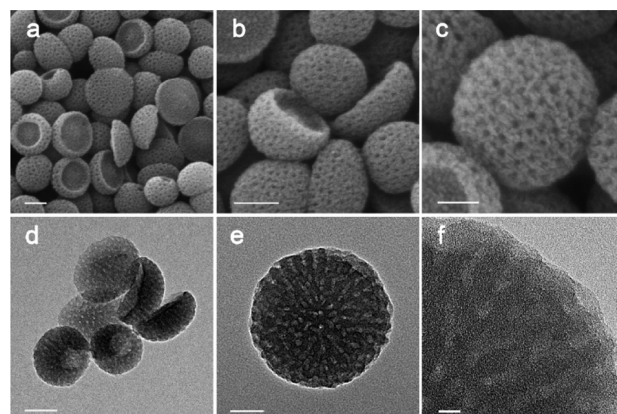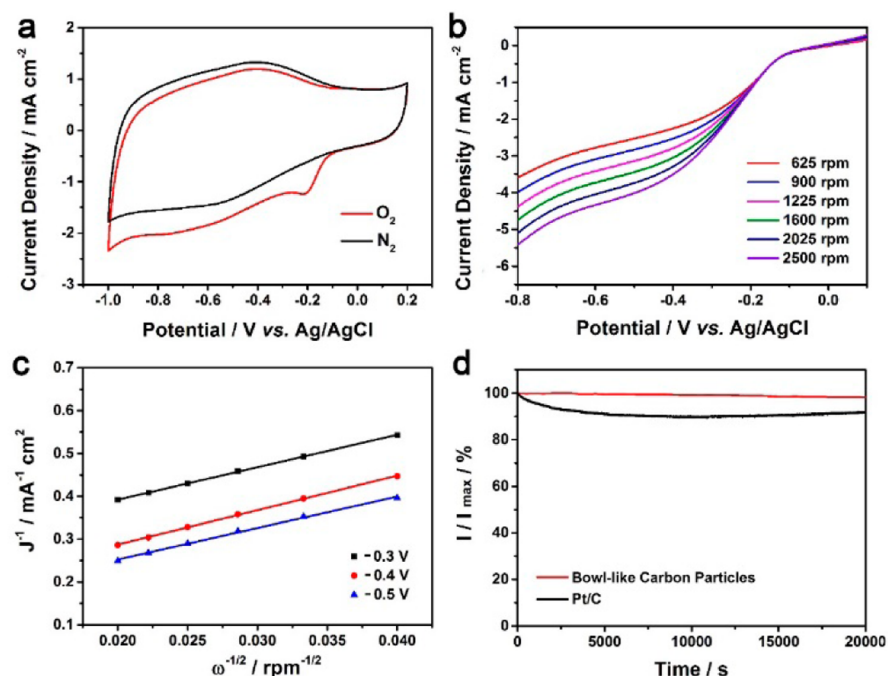

Figure 4. Microscopy characterizations of bowl-like mesoporous carbon particles: (a, b) FESEM images, (c) magnified FESEM image, (d) TEM image, (e) magnified TEM image, and (f) high-resolution TEM image of radially oriented mesochannels in a bowl-like carbon particle. Scale bars are 100 nm (a, b, d), 50 nm (c, e), and 10 nm (f).

(Figure 4a,b) show that the resultant carbon particles preserve the bowl-shaped morphology. At a higher magnification, disordered crumples are observed on the surface of the carbon particles (Figure 4c). As can be observed from the TEM images (Figure 4d,e), the bowl-like carbon particles retain the radially oriented pore structure after the thermal treatment. The smaller mesochannels with diameter of ∼8 nm are formed because of the significant shrinkage of the polymer framework during the pyrolysis at high temperature (Figure 4f). Nitrogen sorption isotherms (Figure S9, SI) show a hysteresis loop, indicating the existence of mesopores. The surface area of these bowl-like mesoporous carbon particles is ∼619 m^2 g^{-1}. The pore size distribution calculated using the Barrett−Joyner−Halenda (BJH) model (inset of Figure S9) shows that the size of the majority of the pores falls in the range of 7−9 nm, which agrees well with that estimated from the TEM images. Energy-dispersive X-ray spectroscopy (EDX) measurement confirms that the annealed carbon particles contain C, N, and O elements (Figure S10, SI).

To demonstrate the application of bowl-like mesoporous carbon particles, we investigate their electrocatalytic properties for ORR. The electrocatalytic activity of the bowl-like mesoporous carbon particles is first examined by cyclic voltammetry (CV) measurements in 0.1 M KOH solution at room temperature. As shown in Figure 5a, no obvious redox peak is observed for bowl-like mesoporous carbon particles in N$_2$-saturated 0.1 M KOH electrolyte. In contrast, when the solution is saturated with O$_2$, a cathodic peak is clearly observed

Figure 5. Electrochemical characterizations of bowl-like mesoporous carbon particles as an electrocatalyst for ORR: (a) CV curves in N_2-saturated and O_2-saturated 0.1 M KOH solution with a sweep rate of 50 mV s^{-1}; (b) LSV curves in O_2-saturated 0.1 M KOH solution with a sweep rate of 10 mV s^{-1} at different rotation speeds ranging from 625 to 2500 rpm; (c) corresponding Koutecky−Levich plots (J^{-1} versus $\omega^{-1/2}$) at different potentials from the LSV curves shown in panel b; (d) durability test in O_2-saturated 0.1 M KOH at −0.5 V.

at −0.21 V versus Ag/AgCl. Linear sweep voltammetry (LSV) measurements at different rotation speeds are further performed to investigate the electrocatalytic activity and kinetics of the bowl-like mesoporous carbon particles in O_2-satuated 0.1 M KOH solution. The ORR onset potential of bowl-like mesoporous carbon particles is around −0.11 V versus Ag/AgCl (Figure 5b). The corresponding Koutecky−Levich (K-L) plots (Figure 5c) show the inverse current density (J^{-1}) as a function of the inverse of square root of the rotating speed ($\omega^{-1/2}$) at different potentials. The number of electrons (n) involved per O_2 in the ORR for the bowl-like mesoporous carbon particles is determined by the K-L equation. The n value is ∼3.5 in the potential range of −0.3 to −0.5 V versus Ag/AgCl, suggesting that the ORR process involves both four-electron and two-electron reactions, which is quite common in N-doped carbon materials.[29] The LSV curves of bowl-like mesoporous carbon particles, symmetric mesoporous carbon spheres, and a commercial Pt/C catalyst (20 wt %; Johnson Matthey) are shown in Figure S11 (SI). The bowl-like mesoporous particles show a higher diffusion-limited current compared with symmetric mesoporous carbon spheres, indicating their better electrocatalytic activity for ORR. Moreover, the bowl-like mesoporous carbon particles and commercial Pt/C catalyst are further compared by testing the methanol crossover via chronoamperometric responses at the potential of −0.5 V in O_2-saturated 0.1 M KOH electrolyte at a rotation speed of 1600 rpm (Figure S12, SI). When methanol is added into the electrolyte, there is an instant drop in the current of the commercial Pt/C catalyst electrode, while the current of the electrode with bowl-like mesoporous carbon particles remains almost unchanged. This indicates that the bowl-like mesoporous carbon particles possess excellent tolerance for methanol. Furthermore, the stability of the bowl-like mesoporous carbon particles and Pt/C catalyst is

investigated at −0.5 V in O_2-saturated 0.1 M KOH solution with a rotation speed of 1600 rpm for 20000 s (Figure 5d). During the period, ∼98% of the initial current density is retained for the bowl-like mesoporous carbon particle electrode, whereas the Pt/C electrode shows a much higher current loss of 10%. The electrocatalytic performance of these bowl-like mesoporous carbon particles is comparable to those of many other metal-free carbon-based electrocatalysts reported in literature (Table S1, SI).

In general, interfacial polymerization of reagents on the surface of emulsion droplets is a relatively complicated process. The interaction between the growth material and droplet template is the dominant factor in determining the growth mode. When the interaction is strong, the growth material can overgrow on the whole droplet surface, leading to formation of a hollow structure. When the interaction is weak, the growth material forms segregated particles despite the presence of emulsion droplets. With moderate interaction between the growth material and droplet template, the growth material forms segregated islands on the droplet to reduce the interface between the material and droplet. That is, once seeds or nuclei are formed on the droplet, it is more favorable for the growth material to further grow on these sites than on the droplet surface.

Similar to other catechol compounds, dopamine can serve as a binding agent for attaching to organic substrate surface.[30] In the present system, block copolymer F127/TMB/polydop-amine composite micelles first form segregated nuclei on each TMB droplet. Therefore, the strategy demonstrated in this work allows anisotropic growth and formation of asymmetric mesostructured particles. Despite the numerous soft-templating methods reported in literature, this is the first demonstration of controllable formation of asymmetric mesoporous particles with radially oriented large mesochannels. Importantly, the

mesoporous polydopamine particles can be further transformed into carbon particles with radially oriented mesochannels through thermal treatment in nitrogen atmosphere.

CONCLUSIONS

In summary, an emulsion-induced interface anisotropic assembly strategy is developed to prepare asymmetric bowl-like mesoporous polydopamine particles with radially oriented large mesochannels. A key feature of the new method is that block copolymer F127/TMB/polydopamine composite micelles serve as the structural units for the effective island nucleation and anisotropic growth on emulsion droplets to form asymmetric mesoporous polydopamine particles. This interfacial interaction-driven approach provides the platform for making many designed asymmetric and symmetric particles. These bowl-like mesoporous polydopamine particles can be easily carbonized into mesoporous carbon particles with unchanged shape and mesostructure. As a demonstration, the as-derived bowl-like mesoporous carbon particles are shown to manifest excellent electrocatalytic activity for oxygen reduction reaction. The present approach offers a new way to fabricate asymmetric mesoporous particles for a wide range of applications.

EXPERIMENTAL SECTION

Synthesis of Bowl-like Mesoporous Polydopamine and Carbon Particles. In a typical reaction, 0.1 g of block copolymer F127, 0.15 g of dopamine hydrochloride, and 0.2 mL of TMB are dispersed in a mixture of 5 mL of water and 5 mL of ethanol by ultrasonication for 2 min to form an emulsion solution. Then 0.375 mL of ammonia is added dropwise to the reaction mixture under stirring. The product of bowl-like mesoporous polydopamine particles are collected by centrifugation after 2 h and then washed with water and ethanol several times. The bowl-like particles are then redispersed in a mixture of 5 mL of water and 5 mL of ethanol and heated in a sealed Teflon-lined autoclave (20 mL in capacity) at 100 °C for 24 h. To prepare bowl-like mesoporous carbon particles, the obtained bowl-like polydopamine particles are heated at 1 °C min^{-1} from room temperature to 300 °C and kept at this temperature for 3 h under nitrogen atmosphere. The temperature is then further raised at 1 °C min^{-1} to 800 °C and kept at this temperature for 2 h.

Materials Characterization. Field-emission scanning electron microscope (FESEM; JEOL-6700F) and transmission electron microscope (TEM; JEOL, JEM-2010) are used to examine the morphology of the samples. The nitrogen sorption measurement is carried out on Autosorb 6B at liquid-nitrogen temperature. The composition of the samples is analyzed by energy-dispersive X-ray spectroscopy (EDX) attached to the FESEM instrument. Thermogravimetric analysis (TGA) is performed on SDT Q600 (TA Instruments).

Electrochemical Measurements. Linear sweep voltammetry (LSV) and chronoamperometry for oxygen reduction reaction (ORR) are conducted on a CHI 660D electrochemical workstation with a conventional three-electrode cell. Platinum and Ag/AgCl (3M KCl) electrodes are used as the counter electrode and reference electrode, respectively. The working electrode is prepared as follows: 1.0 mg of catalyst materials (i.e., bowl-like mesoporous carbon particles or 20 wt % Pt/C) is dispersed in the mixture of ethanol (0.2 mL) and Nafion (5 wt %, 10 μL) under ultrasonication for 30 min. Then, 10 μL of the above suspension is dropped on the polished glassy carbon electrode (5 mm in diameter) and dried at room temperature. The electrochemical measurements are performed in basic solution (0.1 M KOH) saturated with O$_2$ between −0.8 and 0.1 V (versus Ag/AgCl) with a scan rate of 10 mV s^{-1}. The LSV curves for ORR are obtained by the rotating disk electrode (RDE) measurement.

ASSOCIATED CONTENT

Ⓢ Supporting Information

The Supporting Information is available free of charge on the ACS Publications website at DOI: 10.1021/jacs.6b06558.

> FESEM images, TEM images, digital photos, N$_2$ sorption, EDX spectra of polydopamine precursors and their derived carbon products, and detailed electrochemical characterization (PDF)

AUTHOR INFORMATION

Corresponding Author

*E-mail: xwlou@ntu.edu.sg

Notes

The authors declare no competing financial interest.

ACKNOWLEDGMENTS

REFERENCES

(1) Glotzer, S. C.; Solomon, M. J. *Nat. Mater.* **2007**, *6*, 557.

(2) He, J.; Liu, Y.; Hood, T. C.; Zhang, P.; Gong, J.; Nie, Z. *Nanoscale* **2013**, *5*, 5151.

(3) Buck, M. R.; Bondi, J. F.; Schaak, R. E. *Nat. Chem.* **2012**, *4*, 37.

(4) Cortie, M. B.; McDonagh, A. M. *Chem. Rev.* **2011**, *111*, 3713.

(5) Gao, J.; Gu, H.; Xu, B. *Acc. Chem. Res.* **2009**, *42*, 1097.

(6) Cozzoli, P. D.; Pellegrino, T.; Manna, L. *Chem. Soc. Rev.* **2006**, *35*, 1195.

(7) Hyuk Im, S.; Jeong, U.; Xia, Y. *Nat. Mater.* **2005**, *4*, 671.

(8) Li, X.; Zhou, L.; Wei, Y.; El-Toni, A. M.; Zhang, F.; Zhao, D. *J. Am. Chem. Soc.* **2015**, *137*, 5903.

(9) Liang, J.; Hu, H.; Park, H.; Xiao, C.; Ding, S.; Paik, U.; Lou, X. W. *Energy Environ. Sci.* **2015**, *8*, 1707.

(10) Liang, J.; Yu, X.-Y.; Zhou, H.; Wu, H. B.; Ding, S.; Lou, X. W. *Angew. Chem., Int. Ed.* **2014**, *53*, 12803.

(11) Liu, D.; Peng, X.; Wu, B.; Zheng, X.; Chuong, T. T.; Li, J.; Sun, S.; Stucky, G. D. *J. Am. Chem. Soc.* **2015**, *137*, 9772.

(12) Marechal, M.; Kortschot, R. J.; Demirörs, A. F.; Imhof, A.; Dijkstra, M. *Nano Lett.* **2010**, *10*, 1907.

(13) Kim, S.-H.; Hollingsworth, A. D.; Sacanna, S.; Chang, S.-J.; Lee, G.; Pine, D. J.; Yi, G.-R. *J. Am. Chem. Soc.* **2012**, *134*, 16115.

(14) Fang, Y.; Gu, D.; Zou, Y.; Wu, Z.; Li, F.; Che, R.; Deng, Y.; Tu, B.; Zhao, D. *Angew. Chem., Int. Ed.* **2010**, *49*, 7987.

(15) Fang, Y.; Lv, Y.; Gong, F.; Wu, Z.; Li, X.; Zhu, H.; Zhou, L.; Yao, C.; Zhang, F.; Zheng, G.; Zhao, D. *J. Am. Chem. Soc.* **2015**, *137*, 2808.

(16) Wan, Y.; Zhao. *Chem. Rev.* **2007**, *107*, 2821.

(17) Joo, S. H.; Park, J. Y.; Tsung, C.-K.; Yamada, Y.; Yang, P.; Somorjai, G. A. *Nat. Mater.* **2009**, *8*, 126.

(18) Gao, X.; Wu, H. B.; Zheng, L.; Zhong, Y.; Hu, Y.; Lou, X. W. *Angew. Chem., Int. Ed.* **2014**, *53*, 5917.

(19) Chen, Y.; Xu, P.; Chen, H.; Li, Y.; Bu, W.; Shu, Z.; Li, Y.; Zhang, J.; Zhang, L.; Pan, L.; Cui, X.; Hua, Z.; Wang, J.; Zhang, L.; Shi, J. *Adv. Mater.* **2013**, *25*, 3100.

(20) Cao, B.; Yang, M.; Zhu, Y.; Qu, X.; Mao, C. *Adv. Mater.* **2014**, *26*, 4627.

(21) Deng, Y.; Qi, D.; Deng, C.; Zhang, X.; Zhao, D. *J. Am. Chem. Soc.* **2008**, *130*, 28.

(22) Yang, X. Y.; Li, Z. Q.; Liu, B.; Klein-Hofmann, A.; Tian, G.; Feng, Y. F.; Ding, Y.; Su, D. S.; Xiao, F. S. *Adv. Mater.* **2006**, *18*, 410.

(23) Mizoshita, N.; Tani, T.; Inagaki, S. *Chem. Soc. Rev.* **2011**, *40*, 789.

(24) Liu, Y.; Che, R.; Chen, G.; Fan, J.; Sun, Z.; Wu, Z.; Wang, M.; Li, B.; Wei, J.; Wei, Y.; Wang, G.; Guan, G.; Elzatahry, A. A.; Bagabas, A. A.; Al-Enizi, A. M.; Deng, Y.; Peng, H.; Zhao, D. *Sci. Adv.* **2015**, *1*, e1500166.

(25) Han, Y.; Ying, J. Y. *Angew. Chem., Int. Ed.* **2005**, *44*, 288.

(26) Shen, D.; Yang, J.; Li, X.; Zhou, L.; Zhang, R.; Li, W.; Chen, L.; Wang, R.; Zhang, F.; Zhao, D. *Nano Lett.* **2014**, *14*, 923.

(27) Suteewong, T.; Sai, H.; Cohen, R.; Wang, S.; Bradbury, M.; Baird, B.; Gruner, S. M.; Wiesner, U. *J. Am. Chem. Soc.* **2011**, *133*, 172.

(28) Liu, J.; Yang, T.; Wang, D.-W.; Lu, G. Q.; Zhao, D.; Qiao, S. Z. *Nat. Commun.* **2013**, *4*, 2798.

(29) Tang, J.; Liu, J.; Li, C.; Li, Y.; Tade, M. O.; Dai, S.; Yamauchi, Y. *Angew. Chem.* **2015**, *127*, 598.

(30) Lee, H.; Dellatore, S. M.; Miller, W. M.; Messersmith, P. B. *Science* **2007**, *318*, 426.

(31) Peng, Z.; Yang, H. *Nano Today* **2009**, *4*, 143.

(32) Lim, S. I.; Varon, M.; Ojea-Jimenez, I.; Arbiol, J.; Puntes, V. *J. Mater. Chem.* **2011**, *21*, 11518.

(33) Feng, Y.; He, J.; Wang, H.; Tay, Y. Y.; Sun, H.; Zhu, L.; Chen, H. *J. Am. Chem. Soc.* **2012**, *134*, 2004.

(34) Yue, Q.; Wang, M.; Sun, Z.; Wang, C.; Wang, C.; Deng, Y.; Zhao, D. *J. Mater. Chem. B* **2013**, *1*, 6085.